CmaE: A Transferase Shuttling Aminoacyl Groups between Carrier Protein Domains in the Coronamic Acid Biosynthetic Pathway†

Eric R. Strieter, Frédéric H. Vaillancourt,‡ and Christopher T. Walsh*

Department of Biological Chemistry and Molecular Pharmacology, Harvard Medical School, 240 Longwood Avenue, Boston, Massachusetts 02115

Received February 5, 2007; Revised Manuscript Received March 22, 2007

ABSTRACT: During the biosynthesis of the cyclopropyl amino acid coronamic acid from L-*allo*-Ile by the phytotoxic *Pseudomonas syringae*, the aminoacyl group covalently attached to the pantetheinyl arm of CmaA is shuttled to the HS-pantetheinyl arm of the protein CmaD by the aminoacyltransferase CmaE. CmaE will only recognize deacylated CmaA for initial complexation. The aminoacyl group becomes covalently attached to the active site Cys of CmaE and can then be transferred out to the holo pantetheinylated form of CmaD. Both L-Val/L-[^{14}C]Val exchange studies and MALDI-TOF support a reversible shuttling process. Aminoacylated-*S*-CmaE will transfer the L-Val moiety to the HS-pantetheinyl arm of other T domains, including CytC2, BarA, and ArfA C_2-A_2-T_2 but not to free HS-pantetheine. CmaD could be loaded with other amino acids, for example, L-Leu and L-Thr, by the action of heterologous donor T domains containing alternative aminoacyl groups. Additionally, CmaE is able to accept L-Phe as a substrate when presented on CmaD and is able to load this aminoacyl moiety onto heterologous T domains, expanding the potential for CmaE to be used as a tool for generating chemical diversity within an NRPS assembly line.

Many polyketide (PK) and nonribosomalpeptide (NRP) natural products are produced on multimodular, megadalton enzymatic assembly lines (*1*). These modules have core catalytic and carrier protein domains connected *in cis* for efficient sequential passage of the covalently tethered growing acyl chains from one carrier protein domain to the next. However, several variations from the canonical assembly line organization have begun to emerge as more genomes from producer microbes have been sequenced, and biochemical studies on the encoded proteins have been conducted. For example, polyketide synthase (PKS) assembly lines, for example, leinamycin, curacin (*2*−*4*), are known where the core acyltransferase (AT) domains that load malonyl/methylmalonyl CoA monomers are placed *in trans* as free-standing catalysts. The acyl groups are therefore ferried as acyl-O-AT intermediates to the HS-pantetheinyl arm of carrier protein domains that are recognized as acceptor substrates. In the hybrid PKS/NRPS assembly line that makes the siderophore yersiniabactin in the organism *Yersinia pestis*, which causes the plague, the single cysteine-specific adenylation domain acts twice *in cis* within one module and once *in trans* on the other modular protein (*5*).

During recent investigations on the biosynthetic enzymes for syringomycin (*6*), coumermycin (*7*), and coronamic acid (*8*), a new class of *in trans* aminoacyltransferases have been discovered, in which a transferring aminoacyl moiety is shuttled between the HS-pantetheinyl prosthetic groups of donor and acceptor carrier proteins. Because active holo forms of carrier proteins require post-translational installation of the pantetheinyl thiol arm, they are referred to as thiolation (T) domains, and that is the nomenclature used here. In particular, the enzymes for generating 1-amino-1-carboxy-2-ethyl-cyclopropane, coronamic acid, (Scheme 1) from L-*allo*-Ile are encoded by six adjacent genes that activate the amino acid, install it as aminoacyl-*S*-pantetheinyl-T domain (CmaA), chlorinate it on the γ-CH_3 group (CmaB), and then cyclize it to the cyclopropyl scaffold (CmaC) before thioester hydrolysis (CmaT). The functions of the remaining two orfs, CmaD and CmaE, were not immediately obvious: CmaD was predicted to be a free-standing T domain and CmaE a member of the α/β-hydrolase family. It turns out that L-*allo*-Ile-*S*-CmaD but not L-*allo*-Ile-*S*-CmaA is a substrate for the nonheme iron halogenase CmaB, indicating preferential recognition of one T domain scaffold by the halogenase. Our preliminary investigation indicated that CmaE could operate in the system to shuttle the aminoacyl group between the T domains, identifying it as a novel shuttle enzyme for aminoacyl thioesters docked on T domains (*8*).

In this study, we provide further characterization of the activity of CmaE in addition to its ability to recognize different partner proteins and transfer alternative aminoacyl groups. During the shuttling process, CmaE generates a covalent-aminoacyl-*S*-Cys_{105} enzyme intermediate by the

† We gratefully acknowledge the financial support provided in part by the National Institutes of Health Grant GM 20011 (to C.T.W), American Cancer Society Grant PF-05-100-01-CDD (to E.R.S), a Merck-sponsored Fellowship of the Helen Hay Whitney Foundation (to F.H.V.), and a Natural Sciences and Engineering Research Council Postdoctoral Fellowship (to F.H.V.).

* To whom correspondence should be addressed. Tel: 617-432-1715. Fax: 617-432-0438. E-mail: christopher_walsh@hms.harvard.edu.

‡ Present address: Dept. of Biological Sciences, Research and Development, Boehringer Ingelheim (Canada) Ltd., Laval, Qc, H7S 2G5, Canada.

10.1021/bi700243h CCC: $37.00
Published on Web 05/26/2007

Scheme 1: Biosynthesis of the CMA Moiety of Coronatine

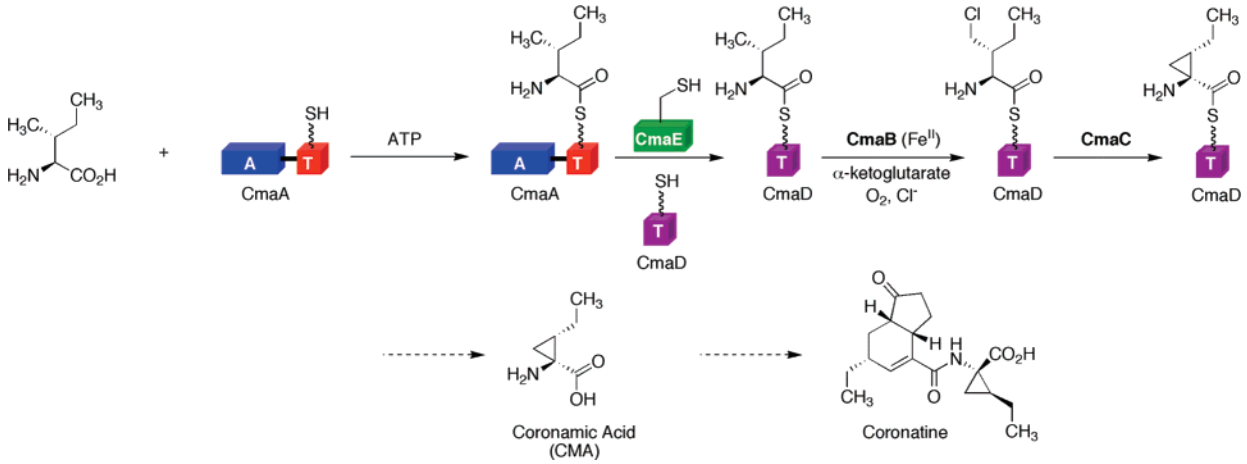

Scheme 2: CmaE-Catalyzed Aminoacyl Group Shuttling between CmaA and CmaD

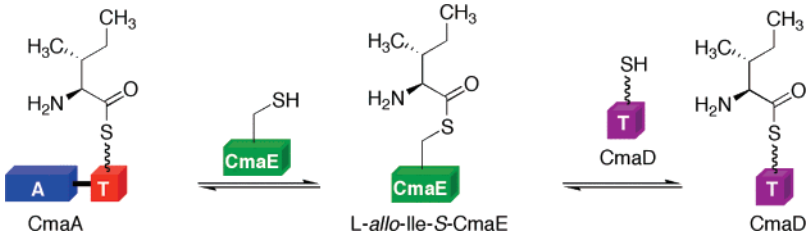

action of its donor substrate L-aminoacyl-*S*-CmaA and delivers it to the sulfhydryl group attached to the phosphopantetheinyl arm on CmaD (Scheme 2). Furthermore, we show that CmaE catalyzes the reverse reaction, in which the aminoacyl group is transferred from CmaD back to CmaA, suggesting that alternative donor/acceptor substrates can be employed. Indeed, CmaE is capable of interacting with heterologous donor and acceptor T domains as evidenced by aminoacyl-*S*-T domain formation through autoradiographic and mass spectrometric analysis. Alternative aminoacyl groups can also be transferred by CmaE, further expanding the repertoire of CmaE beyond that of an aminoacyltransferase subject not only to the coronatine biosynthetic pathway but also to an aminoacyltransferase that can be employed in alternative biosynthetic pathways enabling the generation of further chemical diversity within template-controlled natural product biosynthesis.

MATERIALS AND METHODS

General. Coenzyme A was purchased from MP Biomedicals (Solon, OH). L-Val-*S*-CoA, L-Leu-*S*-CoA, and *N*-Nvoc-L-Phe-*S*-CoA were synthesized as previously described (*9*, *10*). All other chemicals, unless otherwise indicated, were purchased from Sigma-Aldrich. Chemically competent *E. coli* TOP10 and BL21(DE3) cell strains were purchased from Invitrogen. Restriction endonucleases, T4 DNA ligase, and Phusion DNA polymerase were purchased from New England Biolabs. DNA primers for PCR amplification were purchased from Integrated DNA Technologies. The pET28b overexpression vector was purchased from Novagen. Protein concentrations were determined by the method of Bradford, using bovine serum albumin as a standard (*11*). CmaA, CmaE, CmaD, CytC2, BarA, SyrB1, and ArfA C_2-A_2-T_2 were prepared as previously described (*8*, *17*, *19*, *21*, *24*). Autoradiographic analysis was performed on a Typhoon 9410 imager from GE Healthcare. Densitometry was performed using the ImageQuant 5.2 software package from Molecular Dynamics. DNA sequencing and matrix-assisted laser desorption ionization (MALDI) mass spectrometry were performed at the Dana Farber Cancer Institute.

Construction of the Plasmid Encoding CmaA-T. The cmaA-T gene (cmaA containing only the gene encoding the T domain) was amplified from *Pseudomonas syringae* pv. tomato DC3000 (*12*) prepared using the Bactozol kit (Molecular Research Center, Inc.). The following oligo pairs were used for PCR amplification: CmaA-T 5′-GGCAGC**CATATG**TTACAGCCACCGGAGAAAGCAGCGGCGGCGCCC-3′ and CmaA-T 5′-AGCTC**GAATTC**ATCAGTGATTTCC-3′ (*Nde*I and *Eco*RI restriction sites are indicated in bold font). PCR reactions were performed using Phusion DNA polymerase (New England Biolabs) according to the manufacturer's instructions. The resulting amplicons were digested with *Nde*I and *Eco*RI and cloned into pET28b (Novagen). The cloned DNA was sequenced to confirm that no errors were present.

Expression and Purification of Apo-CmaA-T. Escherichia coli BL21(DE3) containing the expression plasmid for CmaA-T was incubated at 37 °C overnight in 60 mL of Luria−Bertani medium (50 μg/mL kanamycin). The following morning, 3 × 20 mL of the overnight culture were used to inoculate 3 × 2 L of Luria−Bertani medium (50 μg/mL kanamycin), and the resulting cultures were grown at 37 °C for 1.5 h (OD_{600} = 0.2). At this time, the temperature was reduced to 15 °C, and the cultures were grown for an additional 2 h prior to the induction of protein expression with the addition of 0.5 mM isopropyl-β-D-thiogalactopy-

ranoside (IPTG[1]). Cultures were incubated for an additional 16 h and then harvested. The harvested cells were resuspended in 100 mL of lysis buffer (25 mM 4-(2-hydroxyethyl)-1-piperazinepropanesulfonic acid (HEPPS) (pH 8.0), 300 mM NaCl, 5 mM imidazole, and 5% glycerol) and lysed by two successive passages through a French press operated at 12,500 psi and 4 °C. The lysates were clarified by ultracentrifugation. The cell-free extract was incubated with 5 mL of Ni-nitrilotriacetic acid (NTA) resin (Qiagen) for 1 h at 4 °C. The resin was washed with an additional 100 mL of lysis buffer and 20 mL of wash buffer (25 mM HEPPS (pH 8.0), 300 mM NaCl, 20 mM imidazole, and 5% glycerol) and eluted with 10 mL of wash buffer containing 200 mM imidazole. The eluates were concentrated using Amicon Ultra centrifugal filter devices (Millipore) containing a cellulose filter with a 5 kDa cutoff and immediately applied to a size exclusion chromatography column equilibrated with 25 mM Hepes (pH 7.5), 50 mM NaCl, and 5% glycerol. The protein fractions were pooled, concentrated to 1.5 mL, and flash-frozen in liquid nitrogen in 10−30 μL aliquots, and stored at −80 °C until further use.

Preparation of Holo-CmaA, CmaA-T, CmaD, CytC2, BarA, ArfA C_2-A_2-T_2, and SyrB1. The priming of the carrier proteins was achieved by incubating the respective protein with surfactin phosphopantetheinyl transferase (Sfp) (*13*) and coenzyme A. A typical priming reaction mixture was incubated at 24 °C for 1 h and contained 100 μM CmaA, 25 mM Hepes (pH 7.5), 5 mM $MgCl_2$, 500 μM coenzyme A, and 1 μM Sfp. The mixture was desalted using a Micro Bio-Spin 6 column (Bio-Rad) and concentrated using an Ultrafree-0.5 centrifugal filter unit (Millipore) to remove excess CoA. In the case where transfer to CytC2, BarA, and ArfA C_2-A_2-T_2 was monitored, the desalting step was not performed.

CmaE Kinetic Assays. The CmaE-catalyzed shuttling of L-[^{14}C]Val from CmaA to CmaD was monitored by SDS−PAGE followed by autoradiography. A typical reaction containing 10 μM *holo*-CmaA, 50 μM *holo*-CmaD, 0.5 μM CmaE, 1.5 mM L-[^{14}C]Val, and 5 mM $MgCl_2$ was initiated by adding 5 mM ATP and quenched at the following time points: 1, 2, 5, 10, and 15 min by mixing with 6× SDS−PAGE protein loading buffer and incubating at 100 °C prior to gel loading. After SDS−PAGE analysis, the proteins were transferred to a PVDF membrane (Bio-Rad) using a Mini-Trans Blot cell (Bio-Rad) operated at 100 V for 45 min with transfer buffer containing Tris base (3.03 g, 25 mmol), glycine (14.41 g, 192 mmol), methanol (200 mL), and H_2O (800 mL). Once the transfer was complete, the membrane was stained and dried prior to exposure to a phosphor storage plate for 12 h. The plates were subsequently imaged using a Typhoon imager (GE Healthcare), and densitometry was performed using ImageQuant 5.2 software (Molecular Dynamics). A standard curve for densitometry was generated by varying the concentration of L-[^{14}C]Val-*S*-CmaA from 0 to 100 μM and comparing the counts obtained from liquid scintillation to the area obtained from densitometry of the autoradiogram.

Initial Velocity Experiments. The initial rate data were simultaneously fit to several kinetic equations for multireactant systems using the least-squares and dynamic weighting options of LEONORA (*14*). The best fit was obtained with the nonlinear steady-state rate eq 1, which describes a ping−pong substituted enzyme mechanism without substrate inhibition, where [A] and [B] are the concentrations of the substrates CmaA and CmaD, respectively, and K_{mCmaA} and K_{mCmaD} are the respective Michaelis−Menten constants.

$$\nu = V_{max}[A][B]/(K_{mCmaD}[A] + K_{mCmaA}[B] + [A][B]) \quad (1)$$

Preparation of L-*Val-S-CmaD*. CmaD was primed by incubating the T domain with Sfp and L-Val-*S*-CoA. In this case, *N*-deprotected L-Val-*S*-CoA could be used directly for loading presumably because the isopropyl group is bulky enough so as to prevent cross-condensation with the amines and the product thioesters. A typical priming reaction was incubated at 24 °C for 1 h and contained 200 μM CmaD, 25 mM Hepes (pH 7.5), 5 mM $MgCl_2$, 500 μM L-Val-*S*-CoA, and 10 μM Sfp. The mixture was desalted using a Micro Bio-Spin 6 column (Bio-Rad).

Preparation of L-*Phe-S-CmaD*. To prime CmaD with L-Phe, *N*-Nvoc-L-Phe-*S*-CoA was used in order to observe successful loading. In a typical reaction, 100 μM of CmaD was added to a mixture of 500 μM *N*-Nvoc-L-Phe-*S*-CoA, 5 mM $MgCl_2$, and 2 μM Sfp. The Nvoc protecting group was subsequently removed by irradiation at 360 nm for 5 min at 4 °C. The mixture was then desalted using a Micro Bio-Spin 6 column (Bio-Rad) and concentrated using an Ultrafree-0.5 centrifugal filter device (Millipore) to afford L-Phe-*S*-CmaD.

MALDI-Time-of-Flight (TOF) Mass Spectrometry. To determine the mass of apo, holo, L-Val-*S*-PCPs, L-Leu-*S*-PCPs, and L-Phe-*S*-PCPs, mass spectrometry analyses on proteins purified using Zip Tip C4 (Millipore) pipet tips were performed with a linear MALDI-TOF mass spectrometer. Samples were prepared by using α-sinapinic acid (10 mg mL^{-1} in 70% acetonitrile/H_2O) as the matrix. Cal3 ($M + H^+$ = 5737.51, 12361.96, and 16952.27 Da) was used for calibration of the instrument, which was performed before each experiment.

RESULTS

CmaE Catalyzes the Transfer of L-*Val from CmaA to CmaD*. In earlier works, CmaE was qualitatively shown to catalyze the transfer of both L-*allo*-Ile and L-Val from CmaA, which is an adenylation carrier protein (A-T) didomain, to the free-standing T domain CmaD (*8*). According to bioinformatic analysis, CmaE belongs to the α/β-hydrolase family of proteins (*15*, *16*), and on the basis of sequence alignment with other known acyltransferases within NRPS pathways, CmaE contains a modified GXCXG motif (GXCXS) harboring the active site cysteine, which is catalytically loaded with L-*allo*-Ile with the aid of a conserved upstream/downstream histidine residue (Figure 1). Consistent with this analysis, the CmaE C105A mutant abolishes all transfer of L-*allo*-Ile from L-*allo*-Ile-*S*-CmaA to *holo*-CmaD (*8*).

[1] Abbreviations: A, adenylation; ATP, adenosine triphosphate; C, condensation; HPLC, high-performance liquid chromatography; IPTG, isopropyl-β-D-thiogalactopyranoside; MALDI-TOF, matrix-assisted laser desorption ionization time-of-flight; PCP, peptidyl carrier protein; Ppant, phosphopantetheine; SDS−PAGE, sodium dodecyl sulfate−polyacrylamide gel electrophoresis; T, carrier protein; TFA, trifluoracetic acid.

```
CmaE(99)....DALVGYCSSAPLALLAAN...CmaE(250)...DPDGQHHDFVDGHERL...
SyrC(161)...AHLMGICAGAVIALSAAA...SyrC(377)...SPSKRHTGAAITNLPF...
CloN7(95)...VYLFGSSGGAVTALVLAA...CloN7(250)..FPG-DHTGFLTESESF...
```

FIGURE 1: Sequence alignment for the set of acyltransferases that are found within NRPS clusters. The GXC/SXG motif and its derivative GXCXS from CmaE are hightlighted along with the downstream histidine residue.

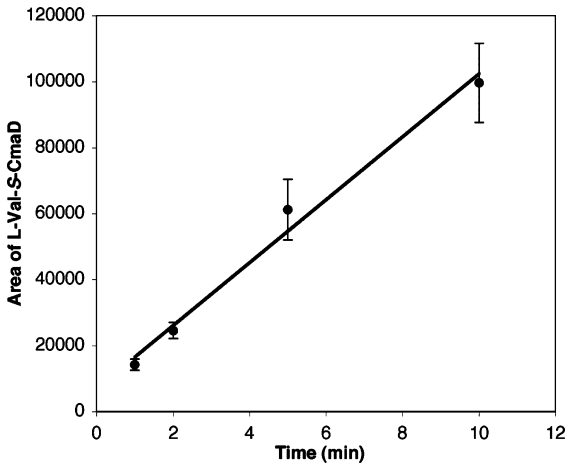

FIGURE 2: Area of L-Val-*S*-CmaD as determined by densitometry of the autoradiogram as a function of time. Conditions: *holo*-CmaA (10 μM), *holo*-CmaD (50 μM), CmaE (0.5 μM), L-[^{14}C]Val (1.5 mM), $MgCl_2$ (5 mM), and ATP (5 mM). Reaction initiated by the addition of ATP and run in triplicate.

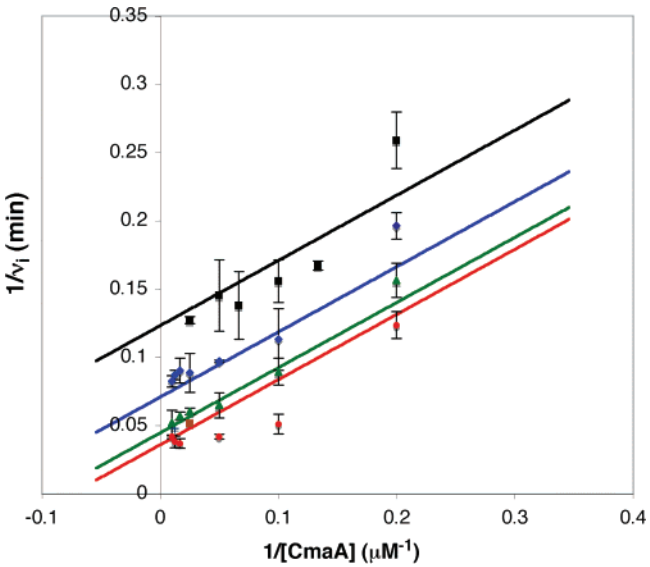

FIGURE 3: Initial velocity patterns for the CmaE catalyzed transfer of L-[^{14}C]Val from CmaA to CmaD as determined by densitometry of the buildup of L-[^{14}C]Val-*S*-CmaD in the autoradiogram (all points were obtained in triplicate). Double reciprocal plot of initial rate data at varying CmaA concentrations and fixed concentrations of *holo*-CmaD at 20 μM (■, black), 40 μM (♦, blue), 80 μM (▲, green), and 120 μM (●, red). The best fit of the data to eq 1 gave kinetic constants of $K_{mCmaA} = 25 \pm 4$ μM, $K_{mCmaD} = 113 \pm 22$ μM, and $k_{cat} = 54 \pm 7$ min^{-1}.

To further characterize CmaE, the steady-state kinetic parameters for the shuttling of L-[^{14}C]Val from CmaA to CmaD were determined by autoradiographic analysis of gel-shift assays. In order to complete this analysis, it was essential for the reactions to be performed with a high concentration of L-[^{14}C]Val (1.5 mM) as this is the concentration at which the adenylation domain of CmaA is saturated, and the autoaminoacylation of *holo*-CmaA goes to completion within 30 s. As shown in Figure 2, the buildup of L-[^{14}C]Val-*S*-CmaD is linear over a period of 10 min, thus allowing for initial velocity measurements. By varying the concentration of *holo*-CmaA (5−100 μM) at fixed concentrations of *holo*-CmaD, a set of parallel lines were obtained in the double reciprocal plot as shown in Figure 3. Using the program LEONORA for data analysis, a best fit to the ping−pong (substituted enzyme) mechanism was obtained with the parameters K_{mCmaA} of 25 ± 4 μM, K_{mCmaD} of 113 ± 22 μM, and a k_{cat} of 54 ± 7 min^{-1}. Although this mechanism may not suit the experimental data, it does however, provide an estimation of the kinetic parameters.

Aminoacylation of CmaE Using CmaA. The first half-reaction was examined in order to gain insight into the rate of aminoacyl group transfer from CmaA to CmaE (see Scheme 2). Previously, we had observed that the thioester that forms upon aminoacylation of the active site cysteine residue is stable enough to detect by autoradiography, suggesting that the aminoacyl-*S*-Cys$_{105}$ enzyme intermediate is impervious to both hydrolysis and nucleophilic attack by the reactive sulfhydryl group from dithiothreitol, which is contained in the quenching buffer. Thus, the buildup of aminoacylated CmaE was followed by autoradiography using L-[^{14}C]Val. As shown in Figure 4A, the aminoacylation of CmaA with L-[^{14}C]Val *prior* to the introduction of CmaE indicated the absence of a L-[^{14}C]Val-*S*-Cys$_{105}$-CmaE enzyme intermediate over the course of 60 min. In contrast, when CmaE was co-incubated with CmaA and L-[^{14}C]Val and the reaction was initiated by the addition of ATP, the L-[^{14}C]-Val-*S*-Cys$_{105}$-CmaE enzyme intermediate was observed to form in a time-dependent fashion as shown in Figure 4B. This intriguing result suggests that CmaE has a greater affinity for the holo (HS-pantetheinyl-) form of CmaA in comparison to that for the aminoacylated (L-Val-*S*-pantetheinyl-) form.

To validate that the labeling of CmaE by the L-[^{14}C]Val group occurs only after incubating CmaE with CmaA, we examined the relative rates of labeling CmaD with L-[^{14}C]-Val as a function of reaction conditions. As shown in Table 1, by adding ATP last to the reaction mixture, the rate of CmaD labeling with L-[^{14}C]Val occurs at an order of magnitude faster than initiating transfer by adding preformed L-[^{14}C]Val-*S*-CmaA (desalted using a Micro Bio-Spin 6 column) to a mixture of CmaE and *holo*-CmaD. This result is congruent with that obtained by examining the first half reaction, providing further evidence that it is essential for CmaE to interact with *holo*-CmaA prior to initiating any aminoacylation event and subsequent aminoacyl group shuttling.

Reversibility of the CmaE-Catalyzed Aminoacyl Group Transfer. To investigate whether CmaE is capable of removing the aminoacyl group from the phosphopantetheinyl arm attached to CmaD and transferring it back to CmaA (see Scheme 2), we first used L-Val-*S*-CmaD in the presence of CmaA, L-[^{14}C]Val, ATP, and CmaE. If the transfer is reversible than CmaE should deacylate the phosphopantetheine arm of CmaD and replace nonradioactive L-Val with

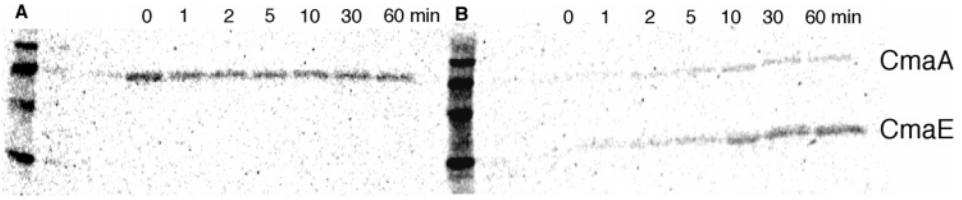

FIGURE 4: Autoradiogram of the aminoacylation of CmaE (5 μM) using CmaA (5 μM), L-[^{14}C]Val (100 μM), ATP (5 mM), and $MgCl_2$ (5 mM) followed over a 60 min time course. (A) CmaA, L-[^{14}C]Val, ATP, and $MgCl_2$ incubated at 25 °C for 30 min prior to the addition of CmaE. (B) ATP added last to a mixture of CmaA, CmaE, L-[^{14}C]Val, and $MgCl_2$.

Table 1: Relative Rates for the Labeling of Holo-CmaD with L-[^{14}C]Val as a Function of Varying Reaction Conditions

reaction conditions	k_{rel}
condition 1: add ATP last to initiate the CmaE-catalyzed transfer from CmaA to CmaD	1
condition 2: add preformed L-Val-S-CmaA to mixture of CmaE and CmaD to initiate the transfer	0.08

Scheme 3: Shuttling of Aminoacyl Groups between Heterologous T Domains Using CmaE

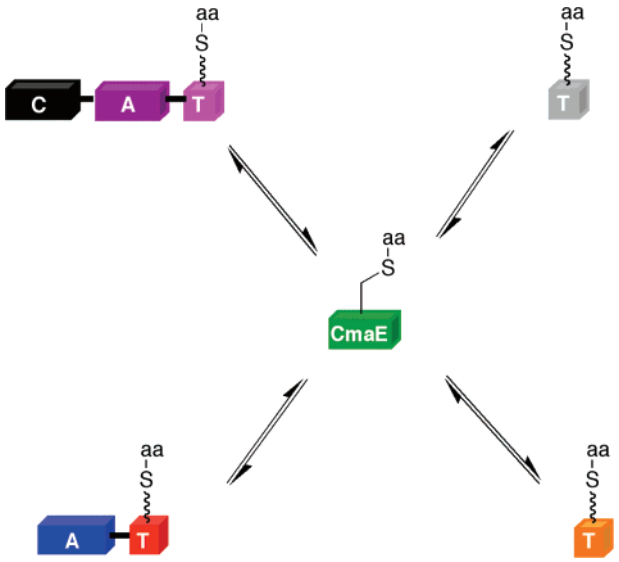

L-[^{14}C]Val in a time-dependent fashion. In order to perform this experiment nonradioactive L-Val-*S*-CmaD was generated by transferring L-Val-*S*-Ppant from L-Val-*S*-CoA through the action of Sfp, a phosphopantetheinyl transferase from *Bacillus subtilis*. The formation of L-Val-*S*-CmaD was verified by MALDI-TOF (10307 $[M + H]^+$ calculated for *apo*-CmaD, 10305 $[M + H]^+$ observed for *apo*-CmaD, and 10747 $[M + H]^+$ calculated for L-Val-*S*-CmaD, 10749 $[M + H]^+$ observed for L-Val-*S*-CmaD). Using L-Val-*S*-CmaD and *holo*-CmaA in an equimolar ratio and adding L-[^{14}C]Val, ATP, and CmaE, we see that the L-Val group on CmaD is indeed replaced by L-[^{14}C]Val in a time-dependent manner, supporting the reversibility of the CmaE-catalyzed aminoacyl transfer (Figure 5).

MALDI-TOF analysis was used to further validate the reversibility of aminoacyl group transfer since the loss of L-Val in the experiment described above could occur as a result of hydrolytic cleavage. In this case, the adenylation domain was removed from CmaA, and the free-standing T domain of CmaA was expressed in *E. coli* and used to examine whether transfer from L-Val-*S*-CmaD to this T domain could occur in the presence of CmaE. As shown in Figure 6 and Table 2, L-Val-*S*-CmaA-T (13226 $[M + H]^+$calculated, 13239 $[M + H]^+$ observed) is formed in the presence of CmaE with the concomitant decrease in mass for L-Val-*S*-CmaD corresponding to the formation of *holo*-CmaD. Furthermore, no peak corresponding to L-Val-*S*-CmaA-T was observed in the spectrum when the inactive CmaE C105A was used in place of CmaE.

Aminoacylation of Heterologous T domains Using CmaA. On the basis of CmaE's ability to catalyze both the forward and reverse aminoacyl transfers with two different T domains, we surmised that CmaE may be capable of utilizing heterologous T domains as donor and acceptor substrates (Scheme 3). Initially, CytC2, a free-standing T domain from the cytotrienin biosynthetic pathway (*17*), was examined as the potential acceptor of L-[^{14}C]Val from CmaA. As shown in Figure 7, CmaE was capable of transferring L-[^{14}C]Val from CmaA to CytC2. In the case of the CmaE C105A active site mutant, labeling of *holo*-CytC2 occurred to a much lesser extent, presumably through a transthioesterification between *holo*-CytC2 and L-[^{14}C]Val-*S*-CmaA. Interestingly, labeling of CmaE occurs to a greater extent than using CmaD, suggesting that CytC2 has a much higher K_m for CmaE. To further expand the scope of CmaE's reactivity, we explored the use of a T domain embedded within a multidomain complex. As shown in Figure 8, CmaE does indeed transfer L-[^{14}C]Val from CmaA to the T domain within ArfA C_2-A_2-T_2, the second module from arthrofactin synthetase (*18*, *19*), and when CmaE C105A is used in place of CmaE, the amount of L-[^{14}C]Val onto ArfA C_2-A_2-T_2 is significantly less. As in the labeling of CytC2, the loading of ArfA C_2-A_2-T_2 occurs with a significant amount of CmaE being labeled by L-[^{14}C]Val, which is again congruent with a higher K_m for heterologous substrates. These results demonstrate that it is possible to use CmaE to shuttle aminoacyl groups to heterologous T domains, thus generating chemical diversity within a multimodular assembly line.

Aminoacylation of Heterologous T domains Using CmaD. To examine whether we could further exploit the ability of CmaE to shuttle aminoacyl groups between free-standing T domains, we examined the transfer of aminoacyl groups from aminoacyl-*S*-CmaD to other T domains, for example, CmaA, BarA (a free-standing T domain from the barbamide biosynthetic gene cluster) (*20*−*22*), and CytC2. In this case, the transfer between T domains was monitored by MALDI-TOF because of the inability to separate the respective T domains by SDS−PAGE. The aminoacylated form of CmaD was generated from the transfer of L-Val-*S*-Ppant to the apo form of CmaD using L-Val-*S*-CoA as previously described. As shown in Table 2, CmaE is capable of catalyzing the transfer of L-Val from CmaD to both *holo*-BarA and *holo*-CytC2 with the concomitant descrease in the intensity for

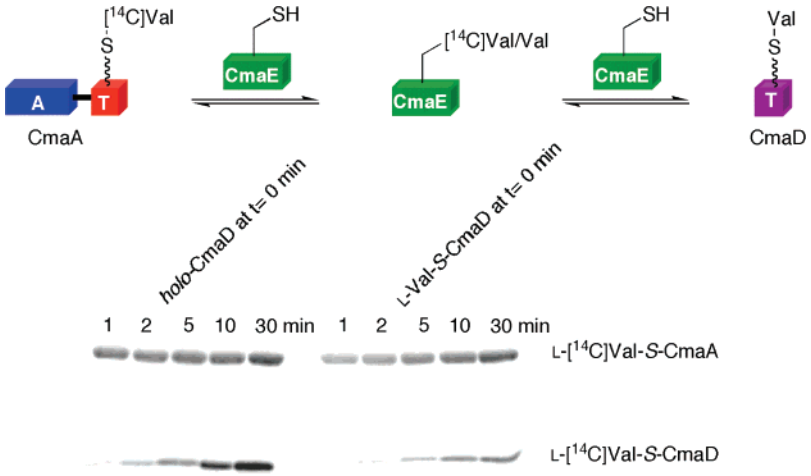

FIGURE 5: L-Val/L-[14C]Val exchange catalyzed by CmaE. Time course for the formation of L-[14C]Val-*S*-CmaD starting from *holo*-CmaD (left side). Time course for the formation of L-[14C]Val-*S*-CmaD starting from L-Val-*S*-CmaD (right side).

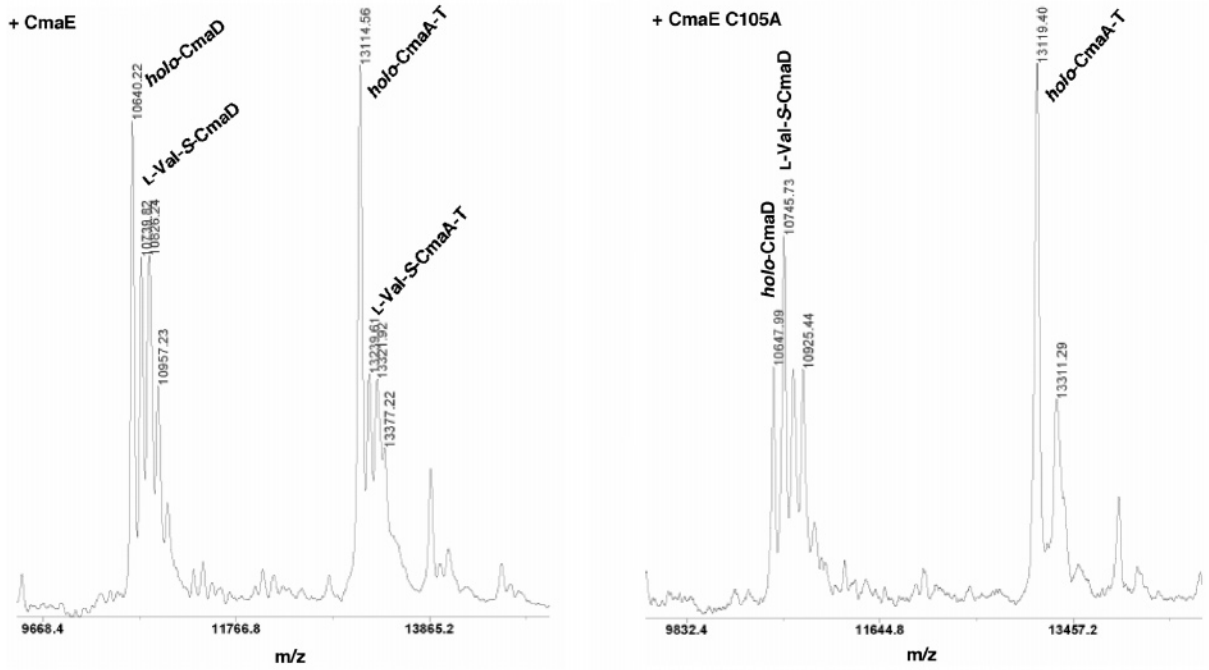

FIGURE 6: MALDI-TOF analysis of the formation of L-Val-*S*-CmaA-T in presence of either CmaE or the active site mutant CmaE C105A.

Table 2: MALDI-TOF Mass Analysis of Holo and Loaded Proteins in the Presence of L-Val-*S*-CmaD and CmaE or CmaE C105A[a]

protein	calculated $[M + H]^+$	observed $[M + H]^+$
holo-CmaA pcp	13126	13116
L-Val-*S*-CmaA pcp	13226	13222
holo-CmaA pcp + L-Val-*S*-CmaD + CmaE		13239, 13120
holo-CmaA pcp + L-Val-*S*-CmaD + CmaE C105A		13119
holo-BarA	13134	13137
L-Val-*S*-BarA	13234	13226
holo-BarA + L-Val-*S*-CmaD + CmaE		13232, 13135
holo-BarA + L-Val-*S*-CmaD + CmaE C105A		13134
holo-CytC2	11794	11794
L-Val-*S*-CytC2	11894	11899
holo-CytC2 + L-Val-*S*-CmaD + CmaE		11903, 11795
holo-CytC2 + L-Val-*S*-CmaD + CmaE C105A		11794

[a] Missing the first methionine.

the mass corresponding to L-Val-*S*-CmaD. However, in each case the reactions were not quantitative as the holo forms of the T domains were still present in the spectrum even at higher concentrations of CmaE. Importantly, L-Val was not transferred to the holo forms of CmaA-T, BarA, or CytC2 when the active site mutant CmaE C105A was used in place of CmaE.

Alternative Aminoacyl Groups. In order to generalize the use of CmaE as an aminoacyl group shuttling agent, we examined whether CmaE could accept other amino acids

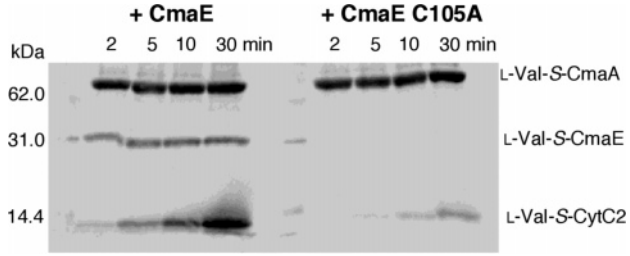

FIGURE 7: Autoradiogram of the CmaE (5 μM) catalyzed transfer of L-[^{14}C]Val (500 μM) from CmaA (10 μM) to CytC2 (50 μM) using $MgCl_2$ (5 mM) and ATP (5 mM).

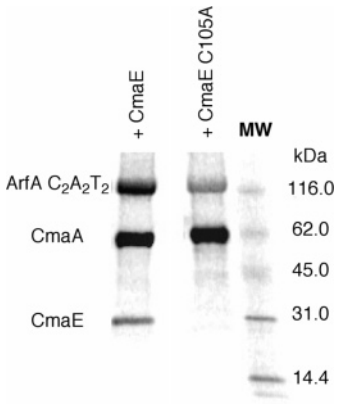

FIGURE 8: Autoradiogram of CmaA (10 μM) and ArfA C_2-A_2-T_2 (20 μM) incubated with L-[^{14}C]Val (500 μM) in the presence of CmaE (lane 1) or CmaE C105A (lane 2) for 60 min.

besides L-*allo*-Ile, its cognate substrate, L-Val, and L-Ile. Because CmaA is ineffective for the activation of other amino acids besides L-*allo*-Ile, L-Ile, and L-Val (*8*), we sought to employ an alternative strategy for determining whether CmaE could accept other aminoacyl groups. In the first case with L-Phe, Sfp was employed to load *apo*-CmaD with *N*-Nvoc-L-Phe-*S*-CoA. The Nvoc-protecting group was subsequently removed through irradiation at 360 nm, thus generating L-Phe-*S*-CmaD, which was confirmed by MALDI-TOF (10794 $[M + H]^+$ calculated, 10802 $[M + H]^+$ observed). As shown in Table 3, the addition of *holo*-CytC2 and CmaE to L-Phe-*S*-CmaD results in the transfer of L-Phe to CytC2. Turning to L-Leu, we used the barbamide synthetase adenylating enzyme, BarD, which activates L-Leu and transfers the activated amino acid to the phophopantetheinyl arm of *holo*-BarA. CmaE does indeed transfer L-Leu from L-Leu-*S*-BarA to CmaD resulting in L-Leu-*S*-CmaD (10760 $[M + H]^+$ calculated, 10756 $[M + H]^+$ observed), whereas with CmaE, C105A L-Leu-*S*-CmaD is not detected (Table 3). Although these results demonstrate that CmaE has the capacity for shuttling nonpolar amino acyl groups of similar structure, the significance resides in the ability to interact with a heterologous donor T domain and a noncognate amino acyl group. Further exemplifying the generality of CmaE's shuttling ability, we examined whether L-Thr could be transferred to CmaD using SyrB1, an adenylation−thiolation didomain from the syringomycin pathway with specificity for L-Thr, as the donor substrate (*23*, *24*). As shown in Figure 9, L-Thr is transferred from SyrB1 to *holo*-CmaD via CmaE in a time-dependent fashion, whereas in the presence of CmaE, C105A transfer to *holo*-CmaD was not observed. Unfortunately, attempts to shuttle L-Thr from SyrB1 to other T domains, that is, CytC2, BarA, or ArfA C_2-A_2-T_2, using CmaE were not successful. Nevertheless, the promiscuity displayed by CmaE in shuttling aminoacyl groups to and from heterologous T domains is promising as an additional strategy for circumventing the specificity of A domains within multimodular NRP megasynthetases.

DISCUSSION

On the basis of exploiting acyl/aminoacyltransferases for creating chemical diversity within NRPS assembly lines, we sought to explore the ability of CmaE, an aminoacyltransferase found within the coronamic acid (CMA) biosynthetic pathway, to serve as a promiscuous shuttling agent. Previously, we have shown that CmaE catalyzes the transfer of a nonproteinogenic amino acyl group, L-*allo*-Ile, from the T domain in CmaA to the free-standing T domain CmaD via an active site cysteine (*8*). Upon aminoacylation of CmaD, the non-heme iron halogenase CmaB chlorinates L-*allo*-Ile in the γ-position, thereby setting the stage for the subsequent cyclopropanation catalyzed by CmaC (Scheme 1). In the present work, we demonstrate that CmaE preferentially interacts with *holo*-CmaA in comparison to aminoacyl-*S*-CmaA and that CmaE is capable of utilizing heterologous donor and acceptor T domains in addition to alternative aminoacyl groups.

The aminoacyl enzyme intermediate of CmaE forms through an active site Cys and is dependent on the chemical state of CmaA, which *holo*-CmaE encounters. As indicated by bioinformatic analysis with other α/β-hydrolases, the side chain −SH of Cys_{105} is a primary candidate for the catalytic nucleophile. Indeed the CmaE C105A mutant is catalytically inactive, and the aminoacyl-*S*-CmaE enzyme intermediate is not observed during aminoacyl group shuttling. Surprisingly, the aminoacyl-*S*-CmaE enzyme intermediate is also absent when *holo*-CmaA is incubated with L-[^{14}C]Val and ATP prior to the introduction of CmaE while monitoring the labeling of CmaE with L-[^{14}C]Val by autoradiography. However, while incubating *holo*-CmaA with CmaE prior to initiating the activation of L-[^{14}C]Val, the formation of L-[^{14}C]-Val-*S*-CmaE was observed to occur in a time-dependent manner. Furthermore, the relative rate is approximately an order of magnitude higher for the loading of *holo*-CmaD with L-[^{14}C]Val when CmaE is incubated with *holo*-CmaA in comparison to that with preforming L-[^{14}C]Val-*S*-CmaA. These results suggest that CmaE recognizes the holo and aminoacylated forms of CmaA in distinct ways. Taking into consideration the recent structural work on the conformational changes that occur when carrier proteins exist in their apo, holo, and acylated forms (*26*−*29*), it is not surprising that CmaE's ability to recognize the T domain of CmaA would be dependent on the conformation in which CmaA resides. Exploration of the CmaA/CmaE recognition dynamics will be the subject of future inquiry.

In a mechanistic context, the observation that CmaE prefers to interact with the holo form of CmaA over the aminoacylated form indicates that binding of CmaE to *holo*-CmaA may precede auto-aminoacylation of CmaA, suggesting that A domains may be regulated by partner proteins. Once CmaA aminoacylates itself, the aminoacyl group is transferred intermolecularly to the Cys_{105} side chain −SH of CmaE. Subsequently, either the conformational change that occurs within CmaE upon aminoacylation or the

Table 3: MALDI-TOF Mass Analysis of Holo and Loaded Proteins in the Presence of CmaE or CmaE C105A[a]

protein	calculated $[M + H]^+$	observed $[M + H]^+$
holo-CmaD	10647	10645
L-Leu-*S*-CmaD	10760	10756
holo-CmaD + BarA + BarD + L-Leu + ATP + CmaE		10756, 10645
holo-CmaD + BarA + BarD + L-Leu + ATP + CmaE C105A		10645
L-Phe-*S*-CmaD	10794	10802
L-Phe-*S*-CytC2	11942	11945
L-Phe-*S*-CmaD + *holo*-CytC2 + CmaE		11948, 11795
L-Phe-*S*-CmaD + *holo*-CytC2 + CmaE C105A		11794

[a] Missing the first methionine.

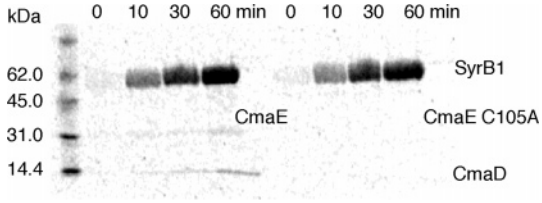

FIGURE 9: Autoradiogram of SyrB1 (20 μM) and CmaD (20 μM) incubated with L-[^{14}C]Thr (200 μM), $MgCl_2$ (5 mM), and ATP (5 mM) in the presence of CmaE (5 μM) or CmaE C105A (5 μM).

regeneration of aminoacyl-*S*-CmaA leads to the dissociation of the CmaA−CmaE complex. For our results to be consistent with the latter hypothesis, a mechanism in which aminoacyl-*S*-CmaA is hydrolyzed after CmaE dissociates, thereby regenerating the CmaE-recognizable holo form of CmaA, would have to occur. Indeed, we have observed that after 5 min of the auto-aminoacylation of CmaA with L-*allo*-[^{3}H]Ile, the amount of aminoacylated CmaA begins to decrease, suggesting that in the absence of CmaE there exists a mechanism by which hydrolysis of the aminoacyl group occurs in a kinetically competent manner (Yeh, E., unpublished results). An alternative mechanism could involve the direct acylation of CmaE by the adenylation domain of CmaA; however, the CmaA S542A mutant, which cannot be phosphopantetheinylated, is unable to facilitate the transfer of L-[^{14}C]Val to CmaD (*8*). Additionally, the acylation of CmaE could induce a conformational change that results in a stabilization of the CmaA−CmaD interaction, thereby facilitating the transthioesterification from one T domain to another; however, further experiments are necessary to delineate this mechanism.

Once CmaE is aminoacylated after initially interacting with *holo*-CmaA, the shuttling of the aminoacyl group to *holo*-CmaD is reversible. More specifically, using both autoradiography and MALDI-TOF mass spectrometry, we established that CmaE is capable of removing the aminoacyl group from CmaD and shuttling it back to CmaA. In the first case, autoradiographic analysis of the L-Val/L-[^{14}C]Val exchange on CmaD indicated that CmaE could catalyze the shuttling of L-Val from CmaD back to CmaA and in turn place L-[^{14}C]-Val onto *holo*-CmaD. This was subsequently validated through MALDI-TOF analysis of the CmaE-catalyzed transfer of L-Val from CmaD to the CmaA-T domain. The combination of these two results reflects CmaE's ability to interact with two T domains whose overall electrostatic properties differ significantly, that is, the pI of CmaD is 4.1, whereas the pI of CmaA-T domain is 5.4. Furthemore, the reversibility of the aminoacylation is consistent with that found in the case of CouN7, a homologue of CmaE, which catalyzes the acetylation/deacetylation of the coumermycin A_1 scaffold (*25*).

Our findings demonstrating the reversible shuffling of aminoacyl moieties to and from cognate T domains suggested that it would be possible to use heterologous T domains as substrates. Along these lines, we first employed CytC2 and BarA, whose identity to CmaD is 16% and 17%, as acceptor substrates. Using CmaA as the donor T domain and L-[^{14}C]-Val as the aminoacyl moiety, CmaE is shown to catalyze the transfer of L-[^{14}C]Val from CmaA to CytC2. In order for the shuttling to these heterologous T domains to be detected, the concentration of CmaE had to be increased by an order of magnitude relative to that when CmaD is used, and the concentration of the acceptor substrate CytC2 had to be in excess of the donor substrate CmaA. The latter two observations are consistent with an increase in K_m for CytC2 relative to CmaD. The next challenge for CmaE occurred with the use of ArfA C_2-A_2-T_2, whose T domain lies at the C-terminus of a three-domain protein. In the event, CmaE also shuttles L-[^{14}C]Val from CmaA to ArfA C_2-A_2-T_2, whereas CmaE C105A does not. This observation is substantial in that it shows that CmaE can be used to transfer an aminoacyl group to a T domain within a large NRPS scaffold, thus offering the opportunity to use CmaE to place alternative aminoacyl moieties within an NRPS assembly line as long as the upstream/downstream condensation domains are able to accept them. Because the K_m for CmaD (113 ± 22 μM) is higher than that for CmaA (25 ± 4 μM), the ability of CmaE to shuttle aminoacyl groups using CmaD as a donor substrate also offers a significant challenge.

Expanding the repertoire of aminoacyl groups that serve as substrates for CmaE is also vital to establish CmaE as a versatile tool in generating chemical diversity within a NRPS assembly line. Thus, we explored whether CmaE could transfer other hydrophobic aminoacyl moieties in addition to L-*allo*-Ile, L-Ile, and L-Val. Both L-Leu and L-Phe could be transferred from a heterologous T domain to CmaD (L-Leu) and from CmaD to a heterologous T domain (L-Phe). Moreover, CmaE transfers L-Thr from SyrB1 to CmaD increasing CmaE's aminoacyl substrate capacity to include those with polar functional groups. Unfortunately, the transfer of L-Thr from SyrB1 to another heterologous T domain such as CytC2, BarA, or ArfA C_2-A_2-T_2 was not successful, presumably because of the high concentrations required of both donor and acceptor substrates. It will, thus, be of interest to understand how CmaE recognizes its donor and acceptor T domains in order to further exploit its utility.

In summary, CmaE joins two other shuttling acyltransferases, SyrC and CouN7, recently identified in NRPS assembly lines (*6*, *7*). The unique chemical logic observed

within the coronatine biosynthetic pathway goes beyond that of a cryptic chlorination pathway and involves the shuttling of aminoacyl moieties to and from T domains. Here, we have shown that CmaE shuttles the aminoacyl group between T domains in a reversible fashion similar to that seen with CouN7. Furthermore, the reactivity of CmaE closely parallels that observed with SyrC and CouN7, where heterologous acceptor (not for SyrC) and donor substrates as well as alternative aminoacyl groups can be employed. Thus, CmaE should be useful for shuttling different aminoacyl groups between T domains existing within heterologous NRPS assembly lines to generate natural product-like derivatives.

ACKNOWLEDGMENT

We thank Dr. Ellen Yeh for her helpful discussions and technical advice concerning CmaE and Dr. Danica P. Galonić for providing BarA and the L-Val-*S*-CoA used in this study. We are also grateful to Mr. Carl J. Balibar for providing the ArfA C_2-A_2-T_2 used in this study and to Dr. Pascal Fortin for his assistance with the program LEONORA.

REFERENCES

1. Fischbach, M. A., and Walsh, C. T. (2006) Assembly-line enzymology for polyketide and nonribosomal peptide antibiotics: logic, machinery, and mechanisms, *Chem. Rev. 106*, 3468−3496.
2. Tang, G.-L., Cheng, Y.-Q., and Shen, B. (2004) Leinamycin biosynthesis revealing unprecedented architectural complexity for a hybrid polyketide synthase and nonribosomal peptide synthetase, *Chem. Biol. 11*, 33−45.
3. Calderone, C. T., Kowtoniuk, W. E., Kelleher, N. L., Walsh, C. T., and Dorrestein, P. C. (2006) Convergence of isoprene and polyketide biosynthetic machinery: isoprenyl-S-carrier proteins in the pksX pathway of *Bacillus subtilis*, *Proc. Natl. Acad. Sci. U.S.A. 103*, 8977−8982.
4. Gu, L., Jia, J., Liu, H., Hakansson, K., Gerwick, W. H., and Sherman, D. H. (2006) Metabolic coupling of dehydration and decarboxylation in the curacin A pathway: functional identification of a mechanistically diverse enzyme pair, *J. Am. Chem. Soc. 128*, 9014−9015.
5. Miller, D. A., Luo, L., Hillson, N., Keating, T. A., and Walsh, C. T. (2002) Yersiniabactin synthetase: a four-protein assembly line producing the nonribosomal peptide/polyketide hybrid siderophore of *Yersinia pestis*, *Chem. Biol. 9*, 333−344.
6. Singh, G. M., Vaillancourt, F. H., Yin, J., and Walsh, C. T. (2007) Characterization of SyrC, an aminoacyltransferase shuttling threonyl and chlorothreonyl residues in the syringomycin biosynthetic assembly line, *Chem. Biol. 14*, 31−40.
7. Garneau-Tsodikova, S., Stapon, A., Kahne, D., and Walsh, C. T. (2006) Installation of the pyrrolyl-2-carboxyl pharmacophore by CouN1 and CouN7 in the late biosynthetic steps of the aminocoumarin antibiotics clorobiocin and coumermycin A1, *Biochemistry 45*, 8568−8578.
8. Vaillancourt, F. H., Yeh, E., Vosburg, D. A., O'Connor, S. E., and Walsh, C. T. (2005) Cryptic chlorination by a non-haem iron enzyme during cyclopropyl amino acid biosynthesis, *Nature 436*, 1191−1194.
9. Sieber, S. A., Walsh, C. T., and Marahiel, M. A. (2003) Loading peptidyl-coenzyme A onto peptidyl carrier proteins: a novel approach in characterizing macrocyclization by thioesterase domains, *J. Am. Chem. Soc. 125*, 10862−10866.
10. Belshaw, P. J., Walsh, C. T., and Stachelhaus, T. (1999) Aminoacyl-CoAs as probes of condensation domain selectivity in nonribosomal peptide synthesis, *Science 284*, 486−489.
11. Bradford, M. M. (1976) A rapid and sensitive method for the quantitation of microgram quantities of protein utilizing the principle of protein-dye binding, *Anal. Biochem. 72*, 248−254.
12. Buell, C. R., Joardar, V., Lindeberg, M., Selengut, J., Paulsen, I. T., Gwinn, M. L., Dodson, R. J., Deboy, R. T., Durkin, A. S., Kolonay, J. F., Madupu, R., Daugherty, S., Brinkac, L., Beanan, M. J., Haft, D. H., Nelson, W. C., Davidson, T., Zafar, N., Zhou, L., Liu, J., Yuan, Q., Khouri, H., Fedorova, N., Tran, B., Russell, D., Berry, K., Utterback, T., Van Aken, S. E., Feldblyum, T. V., D'Ascenzo, M., Deng, W. L., Ramos, A. R., Alfano, J. R., Cartinhour, S., Chatterjee, A. K., Delaney, T. P., Lazarowitz, S. G., Martin, G. B., Schneider, D. J., Tang, X., Bender, C. L., White, O., Fraser, C. M., and Collmer, A. (2003) The complete genome sequence of the *Arabidopsis* and tomato pathogen *Pseudomonas syringae pv.* tomato DC3000, *Proc. Natl. Acad. Sci. U.S.A. 100*, 10181−10186.
13. Quadri, L. E., Weinreb, P. H., Lei, M., Nakano, M. M., Zuber, P., and Walsh, C. T. (1998) Characterization of Sfp, a *Bacillus subtilis* phosphopantetheinyl transferase for peptidyl carrier protein domains in peptide synthetases, *Biochemistry 37*, 1585−1595.
14. Cornish-Bowden, A. (1995) *Analysis of Enzyme Kinetic Data*, Oxford University Press, New York, NY.
15. Holmquist, M. (2000) Alpha/beta-hydrolase fold enzymes: structures, functions and mechanisms, *Curr. Protein Pept. Sci. 1*, 209−235.
16. Nardini, M., and Dijkstra, B. W. (1999) α/β Hydrolase fold enzymes: the family keeps growing, *Curr. Opin. Struct. Biol. 9*, 732−737.
17. Ueki, M., Galonić, D. P., Vaillancourt, F. H., Garneau-Tsodikova, S., Yeh, E., Vosburg, D. A., Schroeder, F. C., Osada, H., and Walsh, C. T. (2006) Enzymatic generation of the antimetabolite γ,γ-dichloroaminobutyrate by NRPS and mononuclear iron halogenase action in a streptomycete, *Chem. Biol. 13*, 1183−1191.
18. Roongsawang, N., Hase, K.-I., Haruki, M., Imanaka, T., Morikawa, M., and Kanaya, S. (2003) Cloning and characterization of the gene cluster encoding arthrofactin synthetase from *Pseudomonas* sp. MIS38, *Chem. Biol. 10*, 869−880.
19. Balibar, C. J., Vaillancourt, F. H., and Walsh, C. T. (2005) Generation of D amino acid residues in assembly of arthrofactin by dual condensation/epimerization domains, *Chem. Biol. 12*, 1189−1200.
20. Chang, Z., Flatt, P., Gerwick, W. H., Nguyen, V.-A., Willis, C. L., and Sherman, D. H. (2002) The barbamide biosynthetic gene cluster: a novel marine cyanobacterial system of mixed polyketide synthase (PKS)-non-ribosomal peptide, *Gene 296*, 235−247.
21. Galonić, D. P., Vaillancourt, F. H., and Walsh, C. T. (2006) Halogenation of unactivated carbon centers in natural product biosynthesis: trichlorination of leucine during barbamide biosynthesis, *J. Am. Chem. Soc. 128*, 3900−3901.
22. Flatt, P. M., O'Connell, S. J., McPhail, K. L., Zeller, G., Willis, C. L., Sherman, D. H., and Gerwick, W. H. (2006) Characterization of the initial enzymatic steps of barbamide biosynthesis, *J. Nat. Prod. 69*, 938−944.
23. Guenzi, E., Galli, G., Grgurina, I., Gross, D. C., and Grandi, G. (1998) Characterization of the syringomycin synthetase gene cluster, *J. Biol. Chem. 273*, 32857−32863.
24. Vaillancourt, F. H., Yin, J., and Walsh, C. T. (2005) SyrB2 in syringomycin E biosynthesis is a nonheme Fe^{II} α-ketoglutarate- and O_2-dependent halogenase, *Proc. Natl. Acad. Sci. U.S.A. 102*, 10111−10116.
25. Balibar, C. J., Garneau-Tsodikova, S., and Walsh, C. T. (2007) A covalent CouN7 enzyme intermediate in coumermycin biosynthesis allows shuttling of acyl groups between aminocoumarin antibiotic scaffolds, *Chem. Biol.*, in press.
26. Koglin, A., Mofid, M. R., Lohr, F., Schafer, B., Rogov, V. V., Blum, M. M., Mittag, T., Marahiel, M. A., Bernhard, F., and Dotsch, V. (2006) Conformation switches modulate protein interactions in peptide antibiotic synthetases, *Science 312*, 273−276.
27. Lai, J. R., Fischbach, M. A., Liu, D. R., and Walsh, C. T. (2006) A protein interaction surface in nonribosomal peptide synthesis mapped by combinatorial mutagenesis and selection, *Proc. Natl. Acad. Sci. U.S.A. 103*, 5314−5319.
28. Lai, J. R., Fischbach, M. A., Liu, D. R., and Walsh, C. T. (2006) Localized protein interaction surfaces on the EntB carrier protein revealed by combinatorial mutagenesis and selection, *J. Am. Chem. Soc. 128*, 11002−11003.
29. Zhou, Z., Lai, J. R., and Walsh, C. T. (2006) Interdomain communication between the thiolation and thioesterase domains of EntF explored by combinatorial mutagenesis and selection, *Chem. Biol. 13*, 869−879.

BI700243H